Placental Imaging: Normal Appearance with Review of Pathologic Findings[1]

Shaimaa Fadl, MD
Mariam Moshiri, MD
Corinne L. Fligner, MD
Douglas S. Katz, MD
Manjiri Dighe, MD

Abbreviations: DWI = diffusion-weighted imaging, IUGR = intrauterine growth restriction, MAP = morbidly adherent placenta, PTN = persistent trophoblastic neoplasia

RadioGraphics 2017; 37:979–998

Published online 10.1148/rg.2017160155

Content Codes: GU MR OB US

[1]From the Departments of Radiology (S.F., M.M., M.D.) and Pathology (C.L.F.), University of Washington Medical Center, 1959 NE Pacific St, Seattle, WA 98195; and Department of Radiology, Winthrop Radiology Associates, Mineola, NY (D.S.K.). Presented as an education exhibit at the 2015 RSNA Annual Meeting. Received June 13, 2016; revision requested August 24 and received October 7; accepted October 24. For this journal-based SA-CME activity, the author M.D. has provided disclosures (see end of article); all other authors, the editor, and the reviewers have disclosed no relevant relationships. **Address correspondence to** M.D. (e-mail: *dighe@uw.edu*).

SA-CME LEARNING OBJECTIVES

After completing this journal-based SA-CME activity, participants will be able to:

- Recognize the normal appearance of the placenta with various imaging modalities.
- Identify common variations and abnormalities seen in the placenta.
- Discuss the added value of cross-sectional imaging in evaluation of trauma, invasive placentation, and gestational trophoblastic diseases.

See www.rsna.org/education/search/RG.

The placenta plays a crucial role throughout pregnancy, and its importance may be overlooked during routine antenatal imaging evaluation. Detailed systematic assessment of the placenta at ultrasonography (US), the standard imaging examination during pregnancy, is important. Familiarity with the normal and abnormal imaging appearance of the placenta along with the multimodality and methodical approach for evaluation of its related abnormalities is necessary, so that radiologists can alert clinicians regarding appropriate prompt management decisions. This will potentially decrease fetal and maternal morbidity and mortality. This article reviews early placental formation and the expected imaging appearance of the placenta during pregnancy, as well as variations in its morphology. It also discusses various placental diseases and their potential clinical consequences. Placental pathologic conditions include abnormalities of placental size, cord insertion, placental and cord location, and placental adherence. Other conditions such as bleeding in and around the placenta, as well as trophoblastic and nontrophoblastic tumors of the placenta, are also discussed. US with Doppler imaging is the initial imaging modality of choice for placental evaluation. Magnetic resonance (MR) imaging is reserved for equivocal cases or when additional information is needed. Computed tomography (CT) has a limited role in evaluation of placental abnormalities because of the ionizing radiation exposure and the relatively limited assessment of the placenta; however, CT can provide important information in specific circumstances, particularly evaluation of trauma and staging of choriocarcinoma. This article also addresses recent techniques and updates in placental imaging, including elastography, diffusion-weighted MR imaging, and blood oxygen level–dependent (BOLD) MR imaging. These advanced imaging techniques may provide additional information in evaluation of abnormal placental adherence and new insights into placental pathophysiology in selected patients.

Online supplemental material is available for this article.

Introduction

The placenta plays a crucial role throughout pregnancy, and its importance may be overlooked during routine antenatal imaging evaluation. Detailed, systematic assessment of the placenta at ultrasonography (US), the standard imaging examination during pregnancy, is important.

In this article, we describe early placental development and its normal anatomic and corresponding imaging appearance. We also discuss different placental pathologic conditions including abnormal morphology, size, and location and abnormal placental adherence, along with trophoblastic and nontrophoblastic placental tumors. Moreover, we describe the characteristic features

TEACHING POINTS

- The term *low-lying placenta* is used when the placental edge is located in the lower uterine segment within 2 cm or less of the internal cervical os; the term *placenta previa* is used when the placental edge covers the internal cervical os. Use of the terms *partial, marginal,* and *complete* is no longer considered acceptable. Accurate measurement of the distance between the lower edge of the placenta and the internal os can be achieved using transvaginal US. A new classification based on transvaginal US according to the placental edge distance from the internal cervical os was proposed recently.
- At gray-scale US, vasa previa appears as linear echolucent structures crossing the cervix. Color Doppler US is the imaging modality of choice and shows vascular structures overlying the internal cervical os with a fixed position during maternal repositioning. Spectral waveforms obtained with Doppler US demonstrate fetal-type flow (with a fetal heart rate) within these vessels.
- Several CT findings should raise concern for placental abruption; one in particular is a full-thickness area of decreased enhancement that forms an acute angle with the myometrium. Hyperattenuating amniotic fluid from placental bleeding into the amniotic cavity may occasionally be seen.
- Gray-scale and color Doppler US are considered the primary diagnostic tools, with overall sensitivity and specificity of 82.4%–100% and 71%–100%, respectively. US features of MAP include an irregular or absent retroplacental clear space at gray-scale US and multiple irregular placental lacunae (Swiss-cheese appearance), with turbulent high-velocity flow deep in the placenta separate from the fetal surface of the placenta.
- Color Doppler US and spectral Doppler waveforms can help differentiate chorioangioma from other placental masses or processes, including placental hemorrhage, hematoma, teratoma, and infarction. Chorioangioma has abundant internal vascularity with low-resistance arterial flow and in some cases may show turbulent venous flow or a single feeding vessel.

of placental abnormalities with several imaging modalities, particularly US and magnetic resonance (MR) imaging. We briefly review the role of computed tomography (CT) in evaluation of the placenta in trauma patients and for staging placental tumors. Finally, we explain several newer techniques for placental imaging, which can provide additional information about placental pathophysiology in selected patients.

Early Placenta Formation

Initially, the blastocyst adheres to the endometrium, and the outer trophoectoderm layer differentiates into syncytiotrophoblasts and cytotrophoblasts (1,2). Syncytiotrophoblasts erode into the endometrial glands and the blood vessels, establishing lacunar networks, which are the primordia of the intervillous spaces of the placenta, whereas cytotrophoblasts form a stem cell column for villous development (Fig 1) (1).

As the chorionic sac grows, the villi associated with the decidua basalis rapidly increase in number, developing a brushy area called the villous chorion (chorion frondosum), which later evolves and forms the placenta (2). The intervillous blood flow is established only after the 12th week of gestation (3), and a slow flow–low impedance uteroplacental circulation is established.

Imaging of Normal Placenta with Different Modalities

Ultrasonography

US is the primary imaging modality of choice for placental assessment in almost all clinical situations. The placenta is visible by 10 weeks gestation at transabdominal US, where it is seen as a thickened echogenic rim of tissue surrounding the gestational sac (4) (Fig 2). Color Doppler imaging can be used to detect intervillous blood flow by 12–14 weeks gestation (Fig 3). Between 12 and 16 weeks gestation, the chorion and amnion fuse.

By 15 weeks gestation, the placenta is well formed and the retroplacental (subplacental) hypoechoic zone is visualized (Fig 4); this is also referred to as the retroplacental clear space. It is the hypoechoic area located behind the placenta, which is composed of decidua, myometrium, and uterine vessels and is 1–2 cm thick. The fetal side of the placenta is called the chorionic plate, and the maternal side is called the basal plate (4).

The normal placenta is discoid with uniform echogenicity and rounded margins. It is usually located along the anterior or posterior uterine walls, extending into the lateral walls. The midportion of the placenta typically measures from 2 to 4 cm. It may show a few focal sonographic lucencies with slow flow, which are called venous lakes. The umbilical cord typically inserts centrally, but marginal and velamentous (within the chorioamniotic membranes) insertions also occur (5).

Increased placental echogenicity can be associated with placental hemorrhage or hypoxia (6,7), while reduced echogenicity and a jelly-like appearance can be associated with preeclampsia (8). The utility of the grading system for placental maturation using US described by Grannum et al (9) has decreased in recent years due to its weak correlation with adverse perinatal outcome; however, premature calcifications may reflect placental vascular insufficiency and may be associated with increased risk of adverse outcome (10).

MR Imaging

MR imaging has the advantage of high soft-tissue contrast resolution; however, it has lower spatial resolution compared with US and therefore is

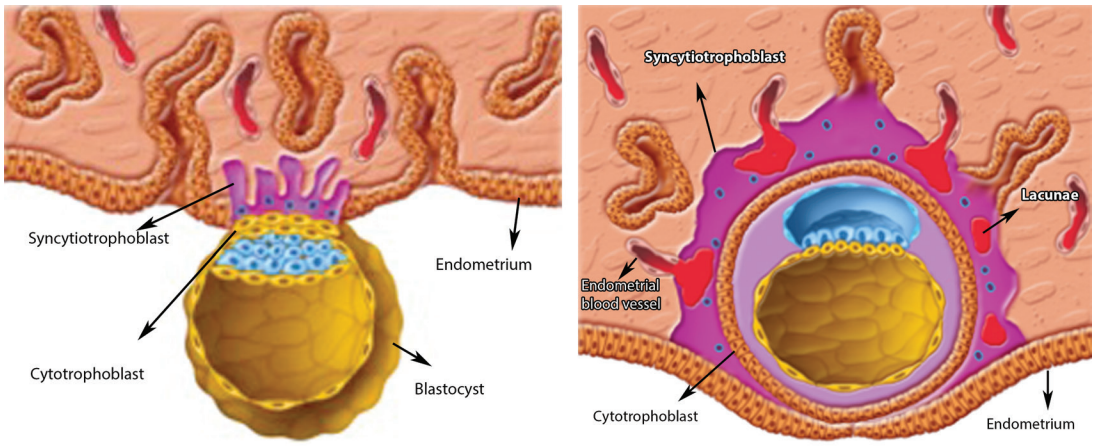

a. **b.**

Figure 1. Early placental development. **(a)** At approximately day 7 after fertilization, the blastocyst attaches to the endometrial epithelium at the embryonic pole of the blastocyst and the syncytiotrophoblast cells start to penetrate and invade the endometrial connective tissue. **(b)** At approximately day 9 after fertilization, the blastocyst implants in the endometrium. Note the formation of extensive syncytiotrophoblasts at the embryonic pole, the start of invasion of endometrial glands, and the formation of lacunae.

Figure 2. Normal placenta at 10 weeks gestation. Transverse gray-scale US image shows the chorion laeve (right arrow) and chorion frondosum (left arrows) of the placenta.

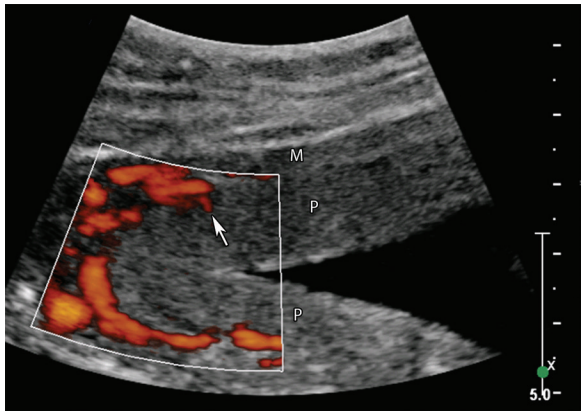

Figure 3. Normal placenta at 12 weeks gestation. Transverse color Doppler image shows intervillous flow (arrow). *M* = myometrium, *P* = placenta.

usually reserved as a complementary technique for equivocal findings at US and/or if additional information is required. The most frequently used sequences for placental evaluation are single-shot fast spin-echo/turbo spin-echo (ssFSE/ssTSE), half-Fourier acquisition single-shot turbo spin-echo (HASTE) T2-weighted, and balanced steady-state free-precession (true FISP [fast imaging with steady-state precession] or FIESTA [fast imaging employing steady-state acquisition]) (11). These sequences usually have the advantage of short timing, with fewer maternal breathing artifacts and fetal movement artifacts (11). A fat-saturated T1-weighted sequence is helpful for detection of blood products (11).

At MR imaging, the normal placenta between 19 and 23 weeks gestation has relatively homogeneous high T2 signal intensity and relatively low T1 signal intensity (Fig 5). Between 24 and 31 weeks gestation, the placenta becomes slightly lobulated and multiple septa between the lobules start to be conspicuous, leading to increased heterogeneity with increasing gestational age (11). The normal myometrium typically appears trilayered on T2-weighted images, with a heterogeneously hyperintense middle layer and thinner low-signal-intensity layers on either side (11). Sometimes, the myometrium appears as a single thin layer of uniform signal intensity at sites of compression, such as adjacent to the spine and aorta (11).

Delineation between the placenta and uterine wall is possible on T2-weighted images (12), where the placenta appears hyperintense relative to the myometrium. This delineation has an important role in cases of morbidly adherent placenta

Figure 4. Normal placenta at 18 weeks gestation. Longitudinal gray-scale US image shows a homogeneous placenta *(P)* with central placental cord insertion *(CI)* and the hypoechoic retroplacental complex (arrows) behind the placenta.

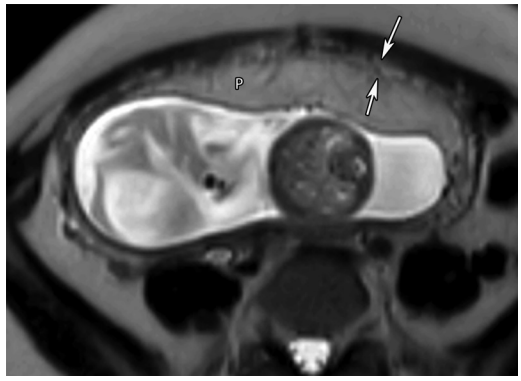

Figure 5. Normal placenta at 19 weeks gestation. Axial T2-weighted MR image shows a homogeneous hyperintense placenta *(P)*. The myometrium is slightly hypointense (arrows) relative to the placenta.

(MAP) (13). MR imaging has the advantage of demonstrating the zonal architecture of the uterus on T2-weighted images, which can be helpful in demonstrating the depth of myometrial invasion in patients with persistent trophoblastic neoplasia (PTN) (14).

Computed Tomography

CT is not routinely used for placental evaluation due to its relatively low tissue contrast resolution and the associated ionizing radiation exposure. However, it may be used in selected circumstances, particularly in trauma and in evaluation of known or suspected metastatic disease related to PTN (15,16). At CT, a normal placenta has a relatively homogeneous appearance that is not clearly distinguishable from the myometrium in the first trimester, but as maturation continues the placenta becomes more heterogeneous (16).

Variations in Placental Morphology

Succenturiate Placenta

A placenta with an accessory lobe is called a succenturiate placenta. At US, the accessory lobe is usually smaller than the main placenta; however, occasionally the accessory lobe is equal in size to the main lobe, which is termed a *bilobed placenta* (5). At US, there is no placental tissue bridging the two placental components. They are connected by intramembranous blood vessels, with the umbilical cord originating from the main placenta (Fig 6, Movie 1).

Succenturiate placenta has an increased risk of vasa previa and rupture of the vessels connecting the lobes during labor, which may lead to fetal death. In addition, there is increased risk of retained placenta, which can result in postpartum hemorrhage (5).

When there is a succenturiate placenta or accessory lobe in the lower part of the uterus, careful evaluation with US for vasa previa and velamentous cord insertion should be performed. Potential mimics of succenturiate placenta at US include uterine contractions and a placenta wrapped around the lateral uterine wall with anterior and posterior components (4). Awareness of these mimics and evaluation with repeat US if necessary can help differentiate an accessory placental lobe from such entities.

Circumvallate Placenta

In a circumvallate placenta, the chorionic membranes do not insert at the edge of the placenta but at some distance inward from the margins, resulting in a rolled up and thickened placental edge and a central depression. This variant may be complete (including the entire placental circumference) or partial. When the placental ring is flat or lacks the central depression, it is called a circummarginate placenta (17). Circumvallate placenta is reported to have an increased risk of chronic placental abruption, preterm delivery,

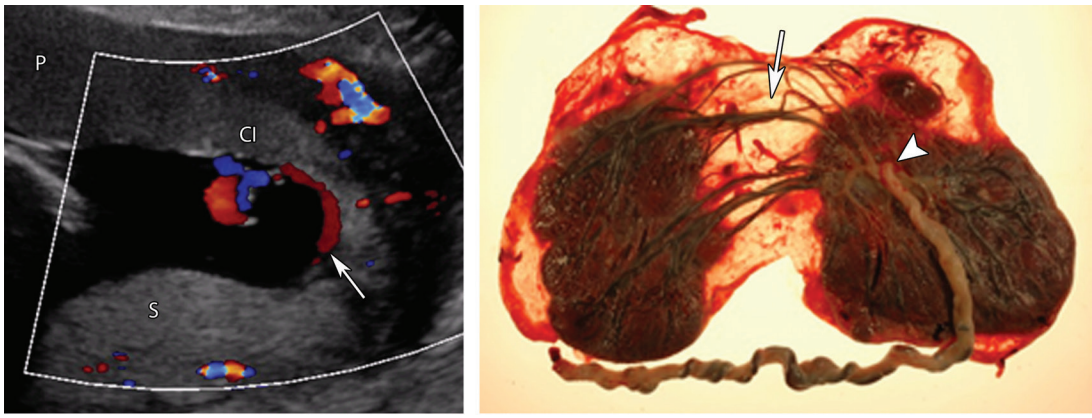

a. b.

Figure 6. Succenturiate placental lobe. **(a)** Longitudinal color Doppler image of a placenta at 24 weeks gestation shows two separate placental lobes, with the placental cord insertion *(Cl)* at the margin of the main lobe *(P)*, near the membranes connecting the lobes. The blood vessels (arrow) are seen traveling from the main lobe and crossing posteriorly toward the succenturiate lobe *(S)*. **(b)** Backlit photograph of a gross specimen from another patient shows two separate placental lobes interconnected by a membrane, with the blood vessels traversing the membranes (arrow). Note the cord origin from the main placental lobe (arrowhead).

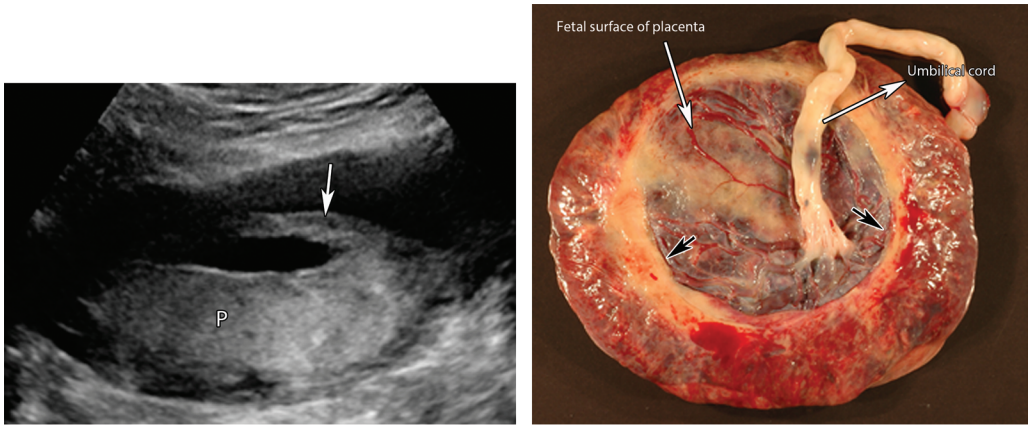

a. b.

Figure 7. Circumvallate placenta. **(a)** Longitudinal gray-scale US image at 21 weeks gestation shows the raised edge of the placenta *(P)* as a linear band of tissue or shelf-like structure (arrow) that may mimic a uterine synechia. **(b)** Photograph of a gross specimen from another patient shows the doubled-back fold in the membranes at their attachment (black arrows) near the margins of the placental fetal surface.

small for gestational age (SGA) status, chronic lung disease (in the child), and neonatal intensive care admissions (18).

At US, the raised edge of the placenta is depicted as a linear band or shelf-like structure isoechoic to the placental tissue. It protrudes toward the amniotic cavity with its base at the placental edge and not attached to any fetal parts (Fig 7, Movie 2). At three-dimensional US, it has been described as analogous to a tire mounted on a wheel (ie, the "tire sign") (19).

Potential mimics of a placental shelf at US include uterine synechiae, amniotic bands, septate uterus, and an old subchorionic hematoma (20). Uterine synechiae may originate from any point of the uterine cavity and may have blood flow. Amniotic bands are thin avascular structures originating from any point of the amniotic surface; either related or unrelated to the placental surface, they may be attached to fetal parts and can cause fetal abnormalities such as limb amputation. Septate uterus is usually recognizable by its fundal position. Old subchorionic hematoma lacks the free margin of the shelf (20,21).

Placenta Membranacea or Diffusa

In placenta membranacea or diffusa, the placenta is a thin membranous structure circumferentially occupying the entire periphery of the chorion. It can be explained by lack of atrophy of the chorionic villi over the amniotic membranes. This is a rare entity. Reported cases were associated with an increased risk of placenta previa, as well as antepartum and postpartum hemorrhage (22).

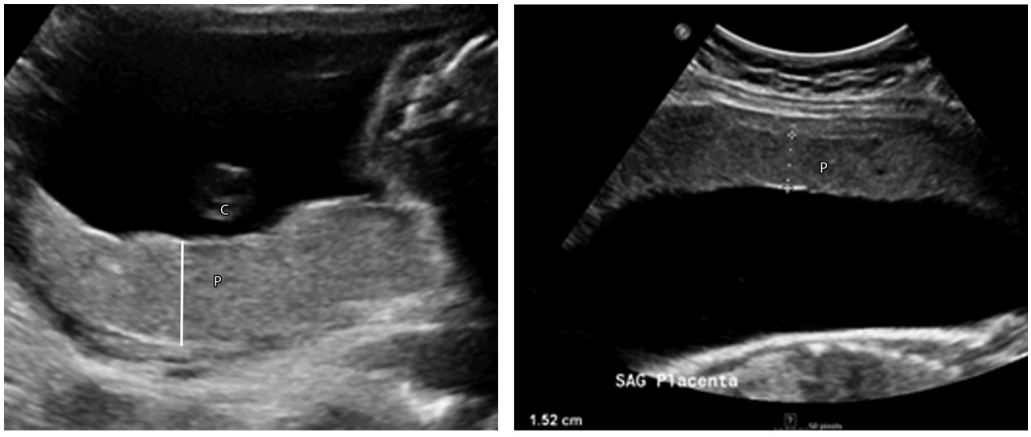

a. b.

Figure 8. Placental thickness. **(a)** Normal placental thickness. Longitudinal US image of a normal placenta at 18 weeks gestation shows the measurement calipers appropriately positioned at the anterior and posterior margins of the placenta *(P)*, perpendicular to the long axis of the placenta near the umbilical cord origin *(C)*. **(b)** Thin placenta. Longitudinal US image of another patient at 30 weeks gestation with polyhydramnios shows a thin placenta *(P)* with a thickness measurement of 1.5 cm (normal at this gestational age = approximately 3 cm).

Placental Thickness

Placental thickness linearly increases with gestational age throughout a normal pregnancy (23,24), with the thickness in millimeters usually correlating with the gestational age in weeks. The average thickness of a normal placenta ranges from 2 to 4 cm. Accurate measurements should be done in the midportion of the placenta near the umbilical cord insertion in cases of central or near-central cord insertion, and must be measured perpendicular to the uterine wall from the subplacental veins to the amniotic fluid, while excluding the myometrium (Fig 8a).

The placental position should be considered when determining placental thickness. Anterior placentas are approximately 0.7 cm thinner than posterior or fundal placentas. An anterior placenta of greater than 3.3 cm and a posterior placenta of greater than 4 cm should be considered thickened (23).

A thickened placenta has been described in association with TORCH infections (*t*oxoplasmosis, *o*ther infections, *r*ubella, *c*ytomegalovirus, *h*erpes simplex), gestational diabetes, and fetal hydrops (23). A thickened placenta with cysts can be seen in partial molar pregnancy, triploidy, and very rarely in placental mesenchymal dysplasia (PMD), which is a rare placental vascular anomaly described in association with Beckwith-Wiedemann syndrome (17).

Placental abruption can be falsely interpreted as a thick placenta when a retroplacental hematoma is isoechoic to the placenta at US (14). Occasionally, uterine contractions or fibroids may mimic a thick placenta. A thin placenta can be related to preeclampsia and intrauterine growth restriction (IUGR) (3) (Fig 8b).

Placental Location

Placental location is determined according to the main placental body position from the uterine equator. It can be anterior or posterior, fundal, or left or right.

The term *low-lying placenta* is used when the placental edge is located in the lower uterine segment within 2 cm or less of the internal cervical os; the term *placenta previa* is used when the placental edge covers the internal cervical os (Fig 9). Use of the terms *partial*, *marginal*, and *complete* is no longer considered acceptable (25). Accurate measurement of the distance between the lower edge of the placenta and the internal os can be achieved using transvaginal US. A new classification based on transvaginal US according to the placental edge distance from the internal cervical os was proposed recently (Table 1) (25).

Transvaginal US is superior to transabdominal US for detection of low-lying placenta (26,27). The benefits of accurate diagnosis with transvaginal US also include screening for MAP and vasa previa, which are strongly associated with placenta previa. The placenta migrates about 1 mm per week (25,28); therefore, the likelihood of a placenta previa diagnosis decreases with gestational age, with a partial previa more likely to resolve than a complete previa (29).

A retrospective study by Dashe et al (29) found that among cases of placenta previa seen at 15–19 weeks, 20–23 weeks, 24–27 weeks, 28–31 weeks, and 32–35 weeks, previa persisted until delivery in 12%, 34%, 49%, 62%, and 73%, respectively, suggesting that previa diagnosed at earlier gestational age has lower incidence of persistence than that diagnosed at later gestational age. Hence, when placenta previa is detected early in pregnancy, fol-

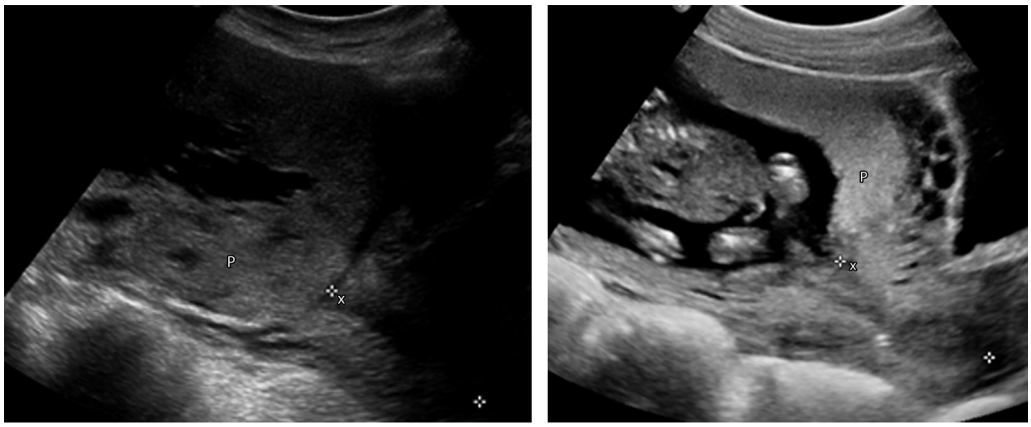

a. **b.**

Figure 9. Placenta previa. **(a)** Complete placenta previa. Longitudinal gray-scale US image at 28 weeks gestation shows the placenta *(P)* completely covering the internal os *(x)*. **(b)** Partial placenta previa. Longitudinal gray-scale US image of another patient at 16 weeks gestation shows a low-lying placenta *(P)* extending to, but not covering, the internal os *(x)*.

Table 1: Classification of Placenta Previa according to Placental Edge Distance from Internal Cervical Os

Placental Edge Distance from Os	Indication for Cesarean Delivery (CD)
>20 mm	Not indicated
11–20 mm	Lower likelihood of bleeding and lower need for CD
≤10 mm	Higher likelihood of bleeding and higher need for CD
Overlap of os by any distance	CD indicated

Source.—Reference 25.

low-up US in the third trimester is recommended to reassess the position of the placenta.

Placental Cord Insertion

The umbilical cord usually inserts in the central portion of the placenta, but sometimes it inserts in an eccentric location, away from the placental edge.

Marginal Cord Insertion

Marginal cord insertion is defined as placental cord insertion within 2 cm of the placental edge (Fig 10). The prevalence of marginal cord insertion is 7%–9% in singleton pregnancies and 24%–33% in twins (30). A study by Liu et al (31) assessed the effect of marginal cord insertion on birth weight and pregnancy duration in singleton pregnancy and concluded that it is not associated with increased risk of growth impairment or preterm delivery. However, marginal cord insertion less than 0.5 cm from the placental edge may progress to velamentous cord insertion later in pregnancy (30,32).

Velamentous Cord Insertion

A velamentous cord inserts into and traverses through the membranes (between the amnion and chorion) before entering the placental tissue (Fig 11, Movie 3). The prevalence of velamentous cord insertion is 1% in singleton pregnancies and about 15% in monochorionic twin gestations (32). Velamentous cord insertion has been associated with low birth weight and an abnormal intrapartum fetal heart rate pattern. In addition, if these vessels overlie the cervix (vasa previa), they may rupture and cause fetal exsanguination.

Vasa Previa

Vasa previa is diagnosed when the umbilical vessels run through the fetal membranes not supported by the placental tissue or Wharton jelly and are close to the internal cervical os and below the presenting part of the fetus. Its prevalence is low, approximately 0.04%, but it carries a significant risk of fetal death when the membranes rupture (33). Early diagnosis of vasa previa, before rupture of the membranes, increases fetal survival from

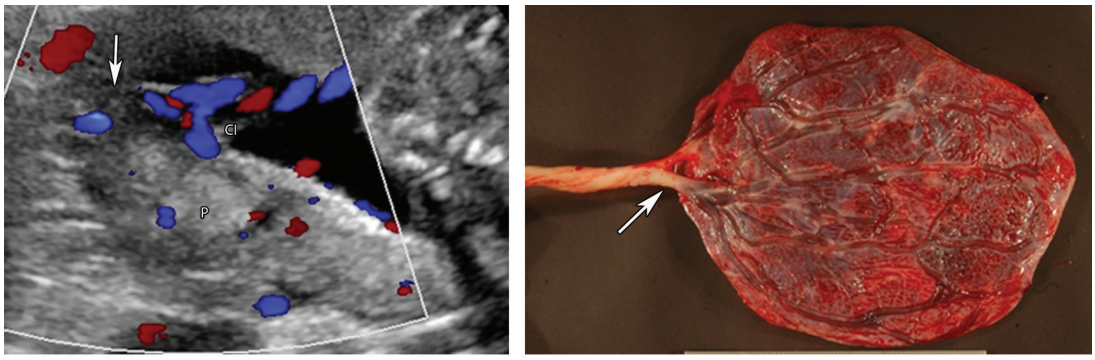

a. b.

Figure 10. Marginal cord insertion. **(a)** Longitudinal color Doppler image at 20 weeks gestation shows placental cord insertion *(CI)* near the margin of the placenta *(P)* within 2 cm of the placental edge (arrow). **(b)** Gross pathology photograph of a placenta from another patient shows marginal cord insertion (arrow). Note the branching vessels over the fetal surface of the placenta.

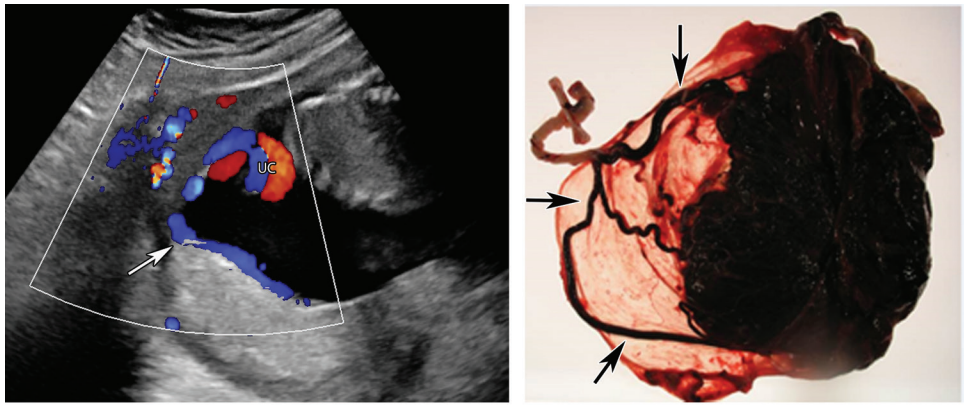

a. b.

Figure 11. Velamentous cord insertion. **(a)** Longitudinal color Doppler image shows a velamentous cord origin. Instead of the umbilical cord *(UC)* inserting into the main placental mass, color flow confirms subtle insertion into the amnion/chorion before insertion into the margin of the placenta (arrow). **(b)** Backlit photograph of a delivered placenta from another patient shows the cord vessels (arrows) traveling between the membranes.

44% to 97%. The key to preventing an adverse fetal outcome is to perform cesarean delivery before rupture of the fetal membranes (34).

At gray-scale US, vasa previa appears as linear echolucent structures crossing the cervix. Color Doppler US is the imaging modality of choice and shows vascular structures overlying the internal cervical os with a fixed position during maternal repositioning (Fig 12). Spectral waveforms obtained with Doppler US demonstrate fetal-type flow (with a fetal heart rate) within these vessels (35).

Mimics of vasa previa include funic presentation, where a loop or loops of a normally inserting umbilical cord precede the presenting fetal part and overlie the internal cervical os. Repositioning the mother during the US examination or serial scans may help differentiate these entities. This maneuver will show movement of the cord loops in a funic presentation. Another potential US mimic is marginal sinus previa, which is described as a discontinuous venous lake at the margin of the placenta (35). Membrane separation and fluid in the membranes below the presenting part are other potential mimics.

Placental Cysts

True cysts, also called chorionic plate cysts, are anechoic thin-walled structures with an estimated prevalence of 2%–7% (5). Such cysts are usually seen along the fetal surface of the placenta, typically near the cord insertion, and demonstrate no internal vascularity at Doppler imaging (Fig 13). They are usually benign and small and frequently go unnoticed; very rarely, if larger than 4.5 cm, they have been reported to be associated with IUGR (17).

Placental lakes or intervillous spaces are usually hypoechoic with swirling echoes and demonstrate low-velocity laminar flow at B-mode or Doppler imaging. They are usually seen in the late second trimester or third trimester. They are

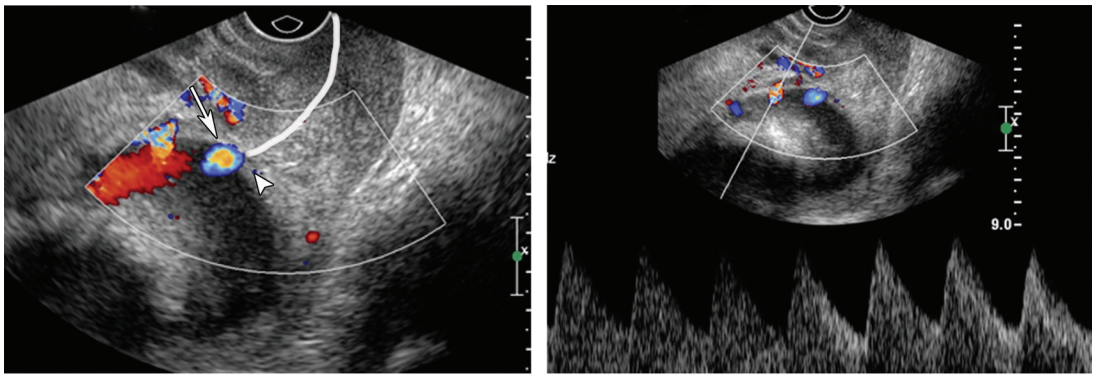

a. b.

Figure 12. Vasa previa. **(a)** Longitudinal transvaginal US image at 33 weeks gestation shows fetal blood vessels (arrow) overlying the internal cervical os (arrowhead). Curved white line = cervical canal. **(b)** Spectral Doppler image shows arterial flow with a fetal heart rate in these vessels, confirming vasa previa.

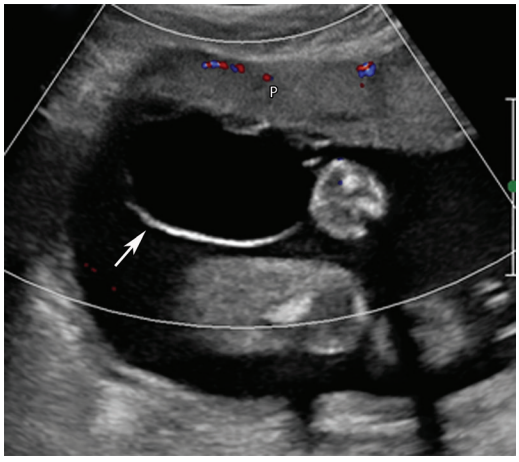

Figure 13. Chorionic plate cyst. Longitudinal color Doppler image at 23 weeks gestation shows a well-defined anechoic avascular structure (arrow) along the fetal surface of the placenta *(P)*, which represents a chorionic plate cyst.

not associated with uteroplacental complications or adverse pregnancy outcomes (36).

Placental Abruption and Associated Hematomas

Placental abruption is defined as premature placental separation from the implantation site. Placental abruption complicates approximately 1% of pregnancies and most frequently occurs between 24 to 26 weeks of gestation (37). Risk factors for abruption include chronic hypertension, trauma, and advanced maternal age (37).

US is insensitive for detection of placental abruption, with reported sensitivity as low as 25% (38). This is because acute and subacute hematomas are frequently isoechoic to placental tissue. US can help determine the extent of abruption by depicting hematomas, which form as a sequela of abruption. A positive finding of a hematoma at US is associated with worse neonatal outcome, since visualization of a blood clot likely indicates a large-volume hemorrhage that would be more likely to manifest signs and symptoms. They also take longer to resorb or drain due to their size (38).

Given that US is not sensitive for detection of abruption, a placental abruption should be considered and treated if clinically suspected regardless of the US findings (38). A prospective study by Masselli et al (39) of 19 patients found MR imaging to be useful and accurate for detection of placental abruption. The authors compared MR imaging and US for detection of abruption and correlated their results with pathologic examination of the placentas. They concluded that MR imaging can accurately depict placental abruption, with excellent interobserver agreement. However, since management of abruption is based on clinical findings, not imaging findings, MR imaging is not routinely performed and can be considered after negative US results if the diagnosis of abruption would potentially change management.

In the setting of trauma to the pregnant patient, the most common injury after solid organ injury is placental abruption. It is crucial for the radiologist to know the normal appearance of the placenta and to recognize placental abruption when evaluating the gravid uterus in a pregnant woman at CT after trauma (40). At CT, the placenta appears homogeneous in the first and early second trimesters, becoming increasingly heterogeneous in the second and third trimesters. Placental cotyledons begin to form in the second trimester and can be seen as foci of rounded low attenuation surrounded by enhancing placenta (16,41). Saphier and Kopelman (42) described a structured descriptive classification of normal and abnormal

Table 2: Traumatic Abruptio Placenta Scale (TAPS) to Describe Placental Appearance after Trauma

Grade	Description
0	Normal homogeneously enhancing placenta
1	Heterogeneous placenta with low-attenuation geographic areas due to normal variants
2	Nongeographic contiguous or full-thickness areas of low attenuation with acute angles with myometrium
2a	>50% placental enhancement
2b	25%–50% placental enhancement
3	Large perfusion defects with <25% overall residual placental enhancement

Source.—Reference 42.

Figure 14. Placental abruption in a 30-year-old woman with profuse vaginal bleeding and a clinical diagnosis of placental abruption after a motor vehicle collision at 28 weeks gestation. Axial contrast-enhanced CT image shows a heterogeneously enhancing placenta with devascularized areas (arrows), which represent areas of infarction. Another small nongeographic area of low attenuation forms an acute angle with the myometrium. More than 50% of the placenta shows enhancement; therefore, this is grade 2a on the Trauma Abruptio Placenta Scale (TAPS).

appearance of the placenta at CT, which they call the Traumatic Abruptio Placenta Scale (TAPS) and which has five grades (Table 2).

In a retrospective study, Wei et al (16) found that interpretation by an experienced CT reviewer for placental abruption after trauma had sensitivity of 100% and specificity of 79.5%–82%, whereas interpretation by less-experienced radiologists had sensitivity of 42.9% and specificity of 89.7% (16). Other studies that examined the performance of CT in diagnosis of placental abruption have also been limited by small number of patients; however, these reported sensitivities of 86%–100% and specificities of 80%–98% when detailed and targeted retrospective analysis was performed (16,43). Several CT findings should raise concern for placental abruption; one in particular is a full-thickness area of decreased enhancement that forms an acute angle with the myometrium (44) (Fig 14). Hyperattenuating amniotic fluid from placental bleeding into the amniotic cavity may occasionally be seen (16).

Pitfalls in CT diagnosis of placental abruption may be seen during the late third trimester, when prominent chorionic indentations may resemble ischemic changes. Myometrial contractions can appear as low-attenuation areas and resemble infarction; however, myometrial contractions have obtuse angles with the adjacent myometrium (16).

Placental hematomas are categorized as periplacental—including subchorionic (preplacental) hematomas (Fig 15) and retroplacental hematomas (Fig 16, Movie 4)—and placental, where the hematoma is centered within the placenta itself (Fig 17). Subchorionic hematomas are the most common type and are usually due to rupture of the uteroplacental veins near the placental margin, with extension between the chorioamniotic membranes and the placenta proper. Retroplacental hematoma is thought to be due to rupture of small decidual arteries and extends between the placenta and uterine wall.

Periplacental and placental hematomas have various appearances at US depending on the stage of bleeding. They tend to be isoechoic acutely, have mixed echogenicity subacutely, then are hypo- to anechoic when chronic, appearing similar to amniotic fluid (5). Retroplacental hematoma should be suspected at US if the retroplacental hypoechoic zone is thickened to more than 2 cm (32). At MR imaging, such hematomas follow the same signal intensity of blood as elsewhere in the body. Mimics at imaging include uterine contractions, which

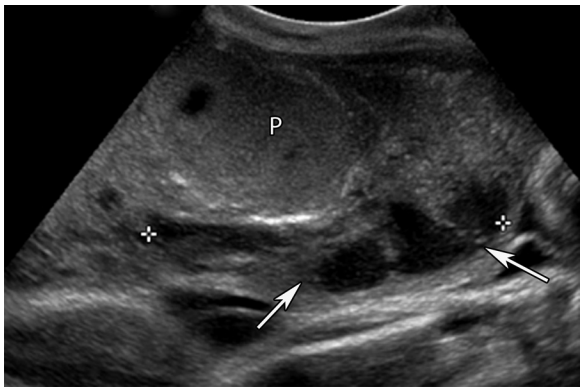

Figure 15. Subchorionic (preplacental) hemorrhage. Oblique gray-scale US image at 32 weeks gestation shows a large heterogeneous crescentic hemorrhage (arrows) between the surface of the placenta *(P)* and the membranes, highly consistent with subacute hemorrhage.

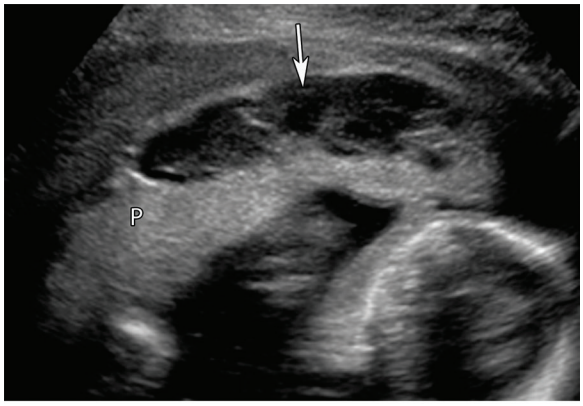

a.

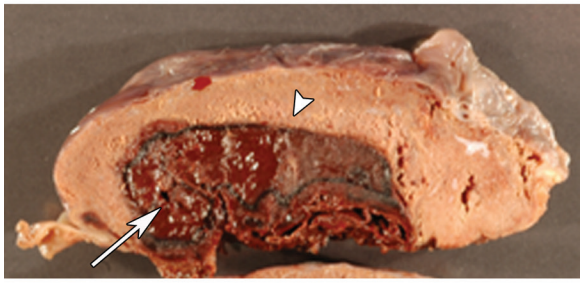

b.

Figure 16. Chronic retroplacental abruption. **(a)** Longitudinal gray-scale US image at 19 weeks gestation shows a hypoechoic to anechoic retroplacental fluid collection (arrow) due to chronic hematoma. *P* = placenta. **(b)** Photograph of the gross specimen from another patient shows a large retroplacental hematoma (arrow) indenting the overlying placental disk (arrowhead).

are usually transient, and uterine fibroids, which demonstrate internal vascularity at color Doppler imaging, whereas hematomas do not (32).

Morbidly Adherent Placenta

MAP is abnormal placental invasion into the uterine wall, leading to failure of placental separation at delivery. The cause of this process is attributed to excessive trophoblastic invasion and defective decidualization (45,46).

The most common risk factors for MAP are prior cesarean delivery and placenta previa. Other risk factors include prior uterine surgery and assisted reproductive techniques (47). The rising incidence of MAP is attributed to the growing rate of cesarean delivery. The risk of MAP is increased with each cesarean delivery (Table 3) (48). Other risk factors include previous myomectomy, advanced maternal age, and Asherman syndrome.

MAP is classified according to the depth of placental invasion into the uterine wall (ie, placenta accreta, increta, and percreta), with increasing degrees of invasion into and outside the uterine wall. In placenta accreta, the placenta is in direct contact with the myometrium; in placenta increta, the placenta invades into the myometrium; and in placenta percreta, the placental invasion extends beyond the uterine serosa and into surrounding structures (45).

Gray-scale and color Doppler US are considered the primary diagnostic tools, with overall sensitivity and specificity of 82.4%–100% and 71%–100%, respectively (11). US features of MAP include an irregular or absent retroplacental clear space at gray-scale US and multiple irregular placental lacunae (Swiss-cheese appearance), with turbulent high-velocity flow deep in the placenta separate from the fetal surface of the placenta (Fig 18, Movie 5) (5,49,50).

An abnormal uterine serosa–bladder interface is reported as the US sign with the highest positive predictive value for MAP (51,52). The normal serosal-bladder interface is an echogenic smooth line without irregularities of vascular signals. Abnormalities of that interface include interruption of the serosal line, thickening of the line, and chaotic vasculature or varicosities.

MR imaging is a complementary imaging examination when US findings are equivocal or the placenta is posteriorly located (13). Overall

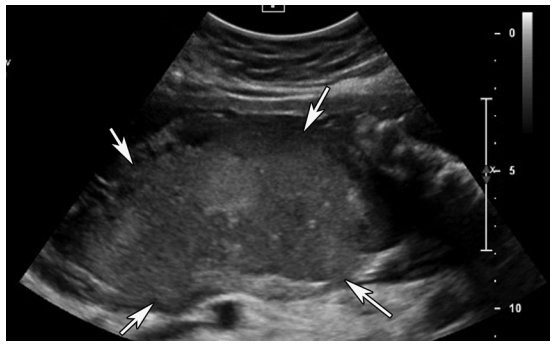

Figure 17. Intraplacental hematoma. Longitudinal gray-scale US image at 27 weeks gestation shows a thick heterogeneous placenta (arrows), which is due to a combination of placental tissue and a large isoechoic acute hematoma.

sensitivity and specificity of MR imaging for this condition are 75%–100% and 65%–100%, respectively (13).

MR imaging findings of MAP include dark intraplacental bands on T2-weighted images, disorganized intraplacental vascularity, abnormal uterine bulge, heterogeneous placenta, thinning or loss of the retroplacental dark zone on T2-weighted images, myometrial thinning or focal disruption of the myometrium, invasion of adjacent organs (particularly the bladder), and tenting of the bladder (Fig 19). Using more than one criterion increases the reliability of the diagnosis. A systematic review by Rahaim and Whitby (13) revealed that the combination of dark bands on T2-weighted images, abnormal uterine bulging, and extremely heterogeneous placenta was consistently associated with MAP and much less frequently seen in normal patients.

Morita et al (53) suggest that diffusion-weighted imaging (DWI) be used as an additional tool for evaluation of placental invasion. DWI at a *b* value of 1000 sec/mm^2 can be helpful for distinction of the border between the myometrium and placenta, as the placenta demonstrates very high signal intensity compared with the adjacent myometrium; thus, focal myometrial thinning caused by placenta increta or percreta can potentially be detected.

Management of MAP requires a multidisciplinary team approach. The ideal management is planned cesarean hysterectomy and avoidance of placental delivery; however, when fertility preservation is desired, other alternative conservative options can be considered, including cesarean delivery combined with temporary aortic balloon occlusion, followed by uterine artery embolization (54,55).

Table 3: Risk of MAP in Patients with Prior Cesarean Deliveries and Placenta Previa

Prior Cesarean Deliveries	Risk of MAP in Patients with Placenta Previa
One	11%
Two	40%
Three	61%

Source.—Reference 48.

Gestational Trophoblastic Disease

Gestational trophoblastic disease (GTD), also termed *molar pregnancy*, includes a wide spectrum of abnormal trophoblastic proliferation. It encompasses complete and partial hydatidiform mole and persistent trophoblastic neoplasia (PTN), which includes invasive hydatidiform mole, placental choriocarcinoma, and placental site trophoblastic tumor.

GTD is a relatively uncommon disease, although the reported incidence rates vary from study to study. It is more common in Asian populations, the reason for which is not fully understood but which may have a genetic basis (56). Markedly increased human chorionic gonadotropin (hCG) secretion is the hallmark of this condition. Enlarged ovaries with multiple theca lutein cysts are seen with hydatidiform moles and coincide with the elevated hCG levels (15).

Complete hydatidiform mole is the most common type of GTD. It has a diploid karyotype 46,XX (usually) or 46,XY. All of the chromosomes are paternal in origin (57), which is probably due to fertilization of an empty ovum by two haploid sperms. It is characterized by diffuse trophoblastic hyperplasia and hydropic swelling of the chorionic villi, with no identified embryonic or fetal tissue.

At US, the endometrial cavity is expanded by hyperechoic or isoechoic tissue with multiple variable-sized cysts, giving the classic "snowstorm" or "clusters of grapes" appearance (Fig 20) (15). During the first trimester, the cysts may be too small to identify at US and the echogenic mass may appear homogeneously solid. No definite blood flow is seen within the molar tissue at color Doppler imaging. No fetus, fetal parts, umbilical cord, or amniotic membranes are identified at US (58).

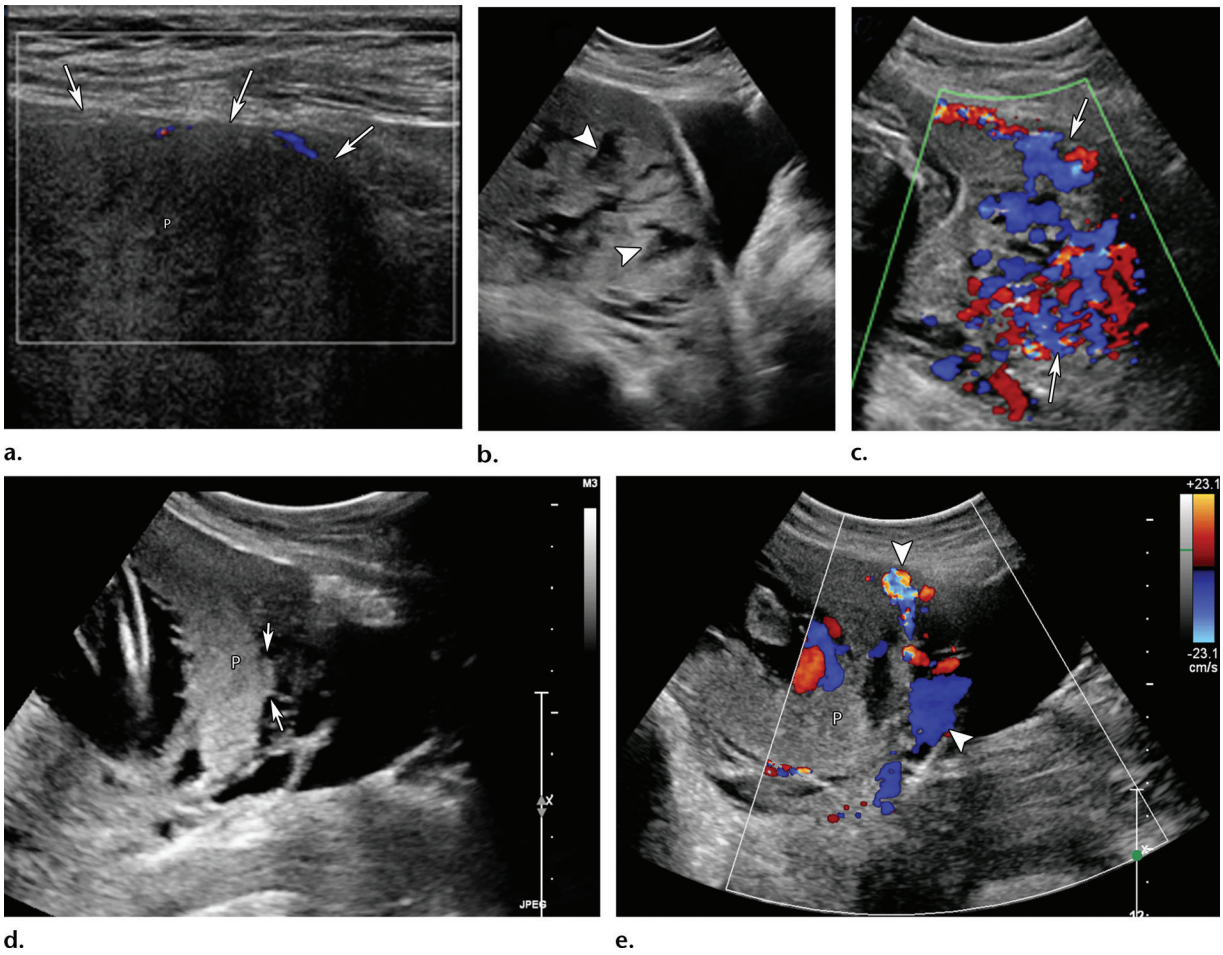

Figure 18. US features of MAP. **(a)** Myometrial thinning. Longitudinal color Doppler image at 28 weeks gestation shows loss of the normal hypoechoic retroplacental space and reduced thickness of the myometrium (arrows) underlying the placenta *(P)*. **(b)** Placental lacunae. Longitudinal gray-scale US image of another patient at 29 weeks gestation shows multiple hypoechoic areas (arrowheads) representing placenta lacunae. These had slow blood flow (not shown). **(c)** Increased vascularity. Longitudinal color Doppler image of placenta increta in another patient at 23 weeks gestation shows increased intraplacental and retroplacental vascularity (arrows). **(d, e)** Loss of bladder–uterine serosal interface. Sagittal gray-scale US **(d)** and color Doppler **(e)** images of another patient at 28 weeks gestation show bulging (arrows in **d**) of the placenta *(P)* and bladder, with increased chaotic vascularity along the interface (arrowheads in **e**).

Partial hydatidiform mole is the second most common type of GTD. It has the triploid karyotype 69,XXY or 69,XYY. It usually develops after fertilization of a normal ovum by two haploid sperms. It is characterized by focal trophoblastic hyperplasia and focal hydropic swelling of the chorionic villi with identified fetal tissue (57).

US shows focal cystic changes of the placenta, and a gestational sac may be seen (Fig 21). When fetal tissue is identified, it is usually abnormal, with only fetal parts instead of a normal fetus or with severe growth restriction or triploid karyotypic congenital anomalies (57). A mimic for partial mole is hydropic degeneration of the placenta; the serum hCG level may help distinguish between the two, since it is lower and progressively decreases in hydropic placental degeneration (58). Another potential mimic is twin pregnancy with a normal-appearing fetus and a concurrent complete molar pregnancy (Fig 22).

PTN includes invasive mole (most common), choriocarcinoma, and rarely placental site trophoblastic tumor. Features that suggest this condition include an hCG plateau level for four consecutive values over 3 weeks or a sequential rise in hCG levels for 2 weeks, persistence of an elevated hCG level 6 months after molar evacuation, histopathologic diagnosis of choriocarcinoma, or metastases (59). The reported incidence of PTN is 18%–29% after a complete mole and 0%–11% after a partial mole (57). US features of PTN include cystic foci or nodules in the myometrium (Fig 23). Hypervascularity and high-velocity, low-impedance arterial flow may be seen at color Doppler imaging (58).

MR imaging has a limited role in GTD; it has no established role in initial diagnosis of hydatidiform mole, to our knowledge, but may be useful in PTN, where it is used for assessment of myometrial invasion and local staging. At MR imaging, a complete hydatidiform mole appears as an

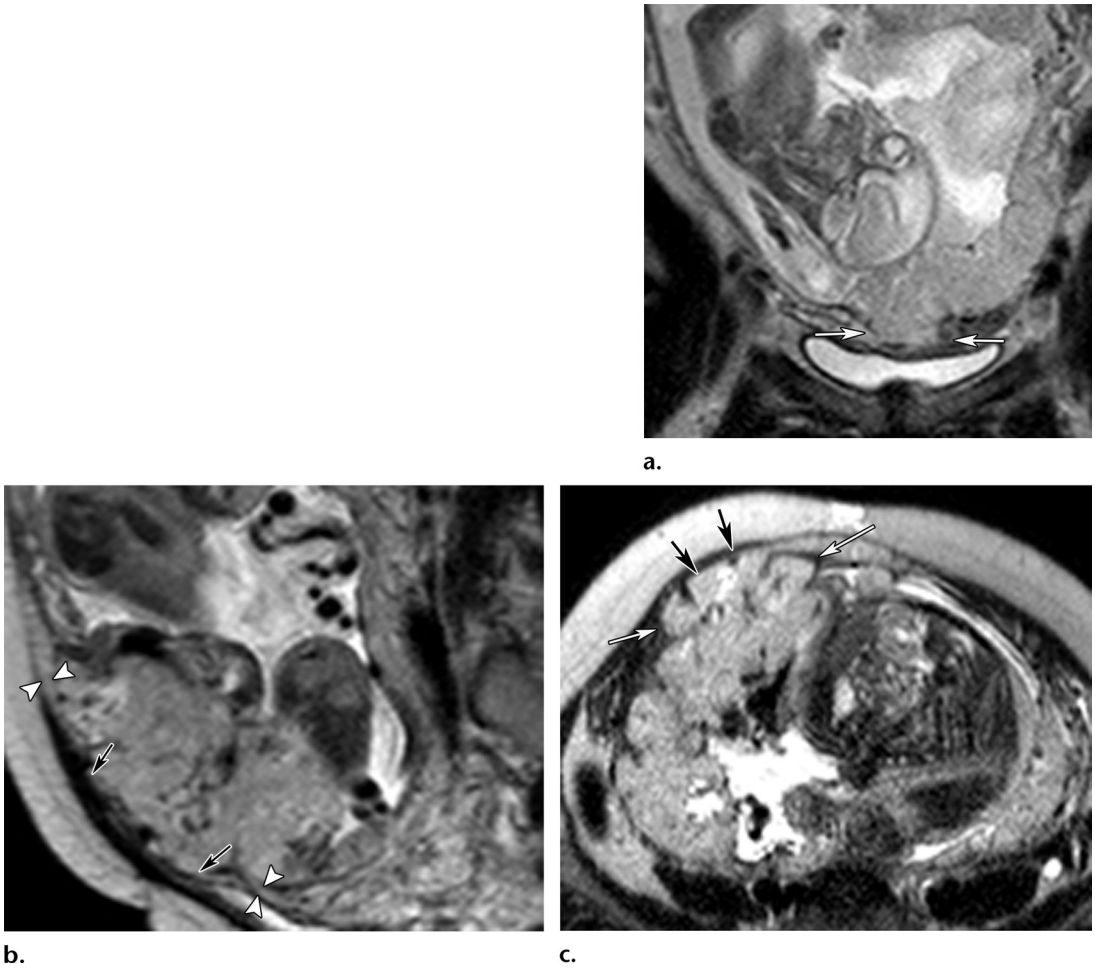

Figure 19. MR imaging features of MAP. **(a)** Placenta increta. Coronal T2-weighted image at 23 weeks gestation shows placenta previa with a focal bulge (arrows) at the lower aspect of the uterus, with discontinuity of the myometrium without bladder-serosa interruption. **(b, c)** Placenta percreta. Sagittal **(b)** and axial **(c)** T2-weighted images of another patient at 26 weeks gestation show a focal placental bulge (white arrows in **c**) at the right anterolateral aspect of the uterus, with discontinuity (black arrows) of the myometrium (arrowheads in **b**).

isointense intracavitary mass on T1-weighted images, is hyperintense on T2-weighted images, has a lattice-like appearance due to cystic changes, and may contain areas of hemorrhage (56). It demonstrates avid gadolinium enhancement and numerous cystic regions. In PTN, particularly invasive mole and choriocarcinoma, the tumor usually has heterogeneous signal intensity on T2-weighted images and an indistinct boundary between the endometrium and myometrium, with either focal or diffuse disruption of the zonal architecture (14) (Fig 24).

In addition, Himoto et al (60) reported that MR imaging allows differentiation between complete hydatidiform mole with coexisting live twin fetus (CHTF) and placental mesenchymal dysplasia (PMD), based on the location of the multicystic mass. In CHTF, the multicystic mass of the complete mole is depicted outside the fetal sac, which contains a normal placenta; however, in PMD the multicystic mass is depicted in the placenta in the fetal sac. The clinical course and pregnancy outcome of these two diseases are different, thus accurate prenatal differentiation is important (60).

CT also has a limited role in diagnosis of molar pregnancy. Its main role is for staging in patients with choriocarcinoma to identify distant metastases.

Placental Nontrophoblastic Tumors

Chorioangioma is the most common nontrophoblastic placental tumor and is identified in 1% of placentas at histopathologic analysis (61,62). Other nontrophoblastic tumors, including teratoma and metastases, are exceedingly rare, with only a few case reports in the literature.

Chorioangioma is a benign vascular tumor supplied by the fetal circulation. Most chorioangiomas are small; however, a minority of chorioangiomas have unpredictable growth and can rapidly increase in size. Large chorioangiomas

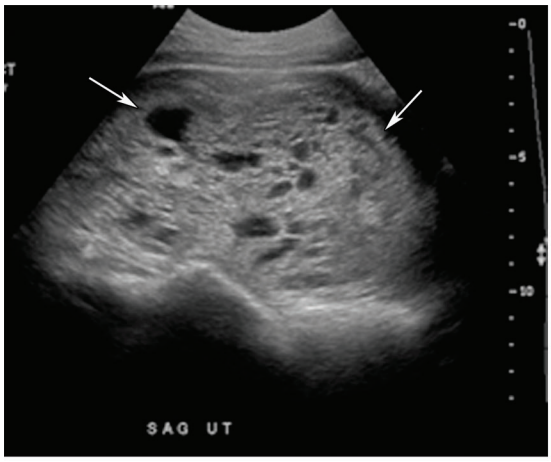

a.

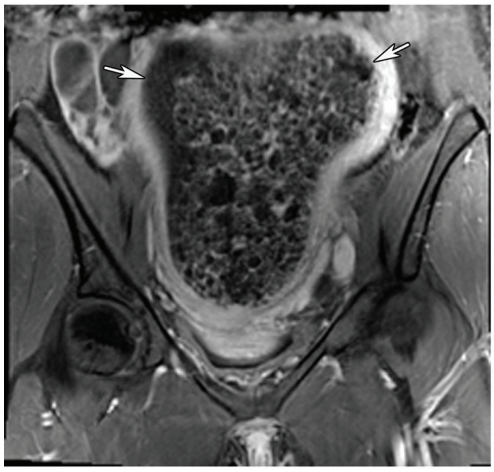

b.

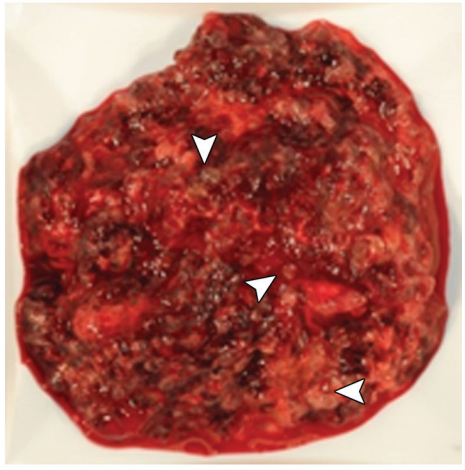

c.

Figure 20. Complete molar pregnancy. **(a)** Longitudinal gray-scale US image shows expansion of the endometrial cavity by a multicystic mass (arrows) (snowstorm appearance). No fetal parts can be identified. **(b)** Coronal gadolinium-enhanced T1-weighted MR image shows expansion of the endometrial cavity (arrows) with lattice-like enhancement of the contents. **(c)** Photograph of the gross specimen shows multiple small cysts (arrowheads) within the mass, representing a complete molar pregnancy.

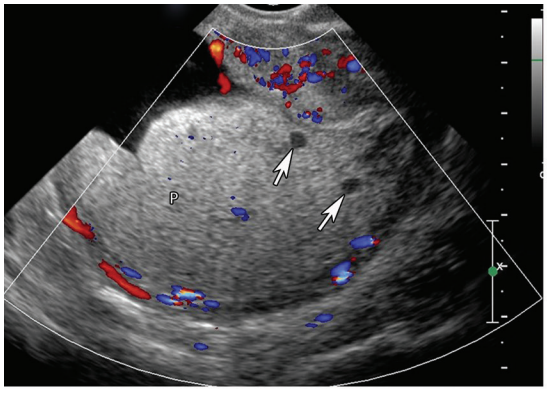

a.

b.

Figure 21. Partial molar pregnancy at 12 weeks gestation. **(a)** Longitudinal color Doppler image shows an enlarged placenta *(P)* containing multiple cysts (arrows). **(b)** Transverse transvaginal US image shows a live embryo, representing a partial molar pregnancy.

greater than 4 cm are uncommon, with a variable prevalence of one in 9000 to one in 16 000 (61,62). At gray-scale US, chorioangioma is seen as a well-circumscribed tumor with mixed echogenicity different from the adjacent placental tissue (Fig 25). Chorioangioma commonly arises from the fetal surface of the placenta near the cord insertion. Tiny calcifications may be seen at US and suggest a favorable prognosis (63–66).

Color Doppler US and spectral Doppler waveforms can help differentiate chorioangioma from other placental masses or processes, including placental hemorrhage, hematoma, teratoma, and infarction. Chorioangioma has abundant internal

Figure 22. Twin pregnancy with a normal fetus and a complete mole, proven at pathologic examination, at 12 weeks gestation in a patient with a history of in vitro fertilization. Longitudinal gray-scale US image shows a normal fetus *(F)* and normal placenta *(P)* in one gestational sac and an abnormally thick placenta *(TP)* with multiple cysts (arrows) in the other gestational sac; the latter represents a complete molar pregnancy. No normal fetal parts are seen in this gestational sac.

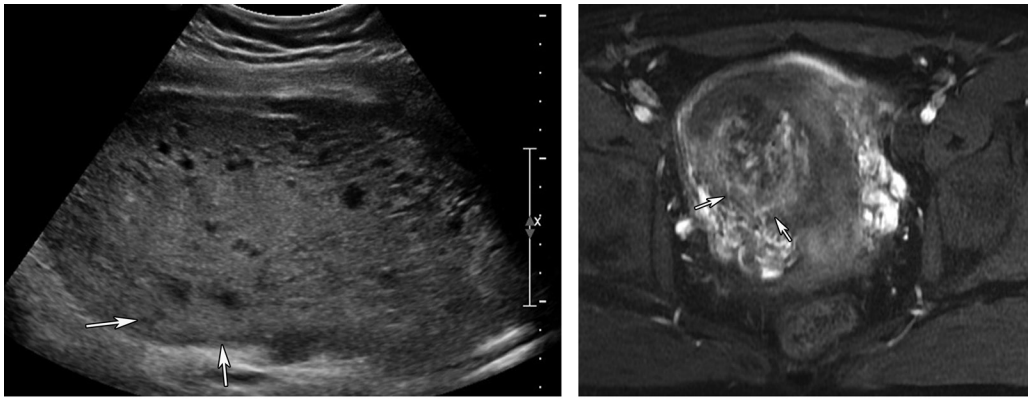

a. **b.**

Figure 23. Invasive molar pregnancy. **(a)** Transverse US image shows an echogenic multicystic mass filling the endometrial cavity. The posterior aspect of the myometrium was not well seen at US (arrows), hence MR imaging was performed. **(b)** Axial contrast-enhanced T1-weighted image shows invasion into the myometrium (arrows), confirming the diagnosis of invasive molar pregnancy.

vascularity with low-resistance arterial flow and in some cases may show turbulent venous flow or a single feeding vessel (64).

Large chorioangiomas are associated with high fetal morbidity and mortality of up to 30%–40% (65). Fetal complications include polyhydramnios, fetal anemia, and fetal hydrops. Serial follow-up monitoring with US and fetal echocardiography should be performed throughout the pregnancy to evaluate the timing of delivery or the need for therapeutic reduction amniocentesis or intrauterine blood transfusion if polyhydramnios or fetal anemia develops (65). US-guided interstitial laser therapy has been described to treat patients with giant chorioangiomas that have caused fetal compromise due to high-output cardiac failure. The main target of the laser therapy is to devascularize the tumor (65).

Placental teratoma is a rare tumor composed of all three germ cell layers. It has been described as benign and is essentially never associated with congenital abnormalities in the fetus. The US features of this tumor include a placental soft-tissue mass of varied echogenicity due to calcifications, fat, and fluid, but without a fetal pole or an umbilical cord insertion (67).

Maternal melanoma has been reported as the most common tumor to metastasize to the placenta. Lung cancer, leukemia, lymphoma, breast cancer, and sarcoma are other malignancies that have rarely been reported to metastasize to the placenta (68).

Recent Techniques and Updates in Placental Imaging

Several relatively new imaging techniques have been used recently to evaluate the placenta. These include US techniques such as elastography, and MR imaging techniques including arterial spin-labeling (ASL), diffusion-weighted imaging (DWI), and blood oxygen level–dependent (BOLD) imaging.

Elastography assesses the stiffness within tissues and has been used in evaluation of multiple organs with both MR imaging and US. Studies on the human placenta suggest that IUGR placentas may have different mechanical proper-

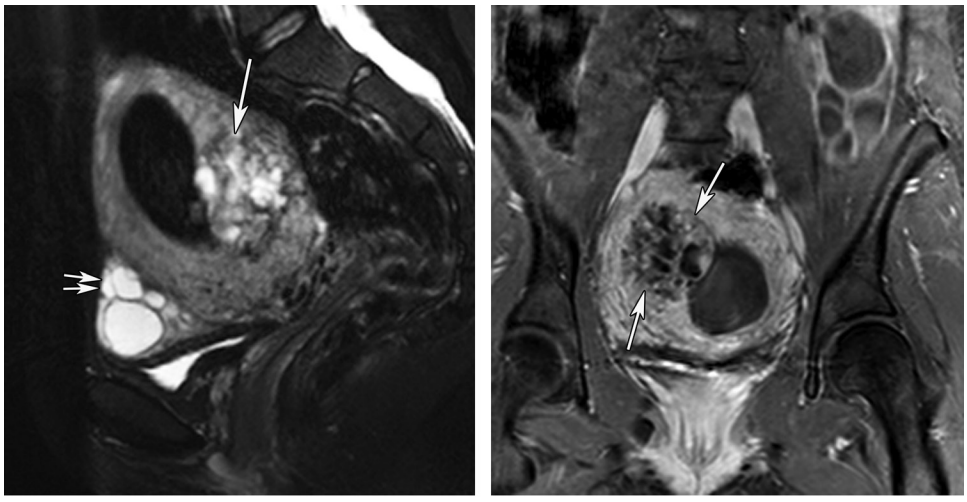

a. b.

Figure 24. Invasive molar pregnancy at 10 weeks gestation. **(a)** Sagittal T2-weighted image shows a large mixed solid and cystic mass (long arrow) extending from the endometrium into the myometrium. Note the multiple theca lutein cysts in the ovaries (short arrows). **(b)** Axial (through the uterus) contrast-enhanced T1-weighted image with fat suppression shows a heterogeneously enhancing mass (arrows) extending from the endometrium into the myometrium.

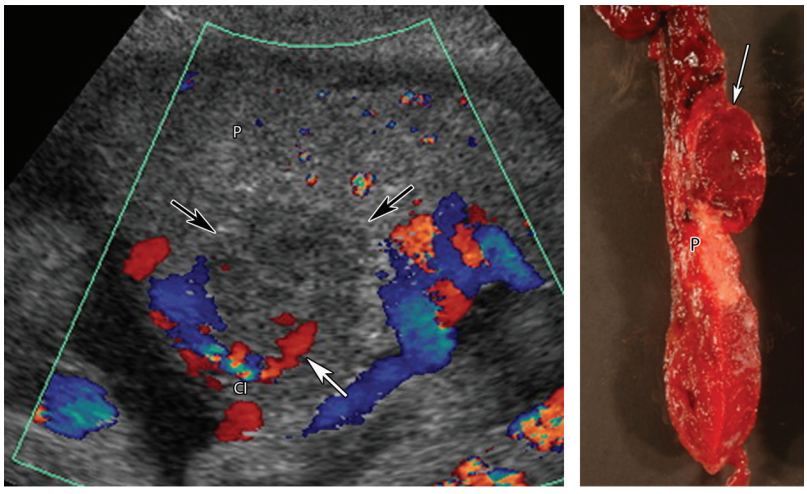

a. b.

Figure 25. Chorioangioma at 32 weeks gestation. **(a)** Longitudinal color Doppler image shows a well-circumscribed hypoechoic mass (black arrows) arising from the fetal surface of the placenta *(P)* adjacent to the cord insertion *(Cl)*. It demonstrates internal vascularity and a large feeding vessel (white arrow). **(b)** Cut section of the delivered placenta from another patient with chorioangioma. Note the reddish mass (arrow) in the placenta *(P)*.

ties than normal placentas. Wu et al (69) found that the shear wave velocity of normal placenta is 0.983 m/sec ± 0.260, with little variation between the second and third trimesters.

Sugitani et al (70) analyzed ex vivo placentas for the velocity of shear wave propagation, using an acoustic radiation force impulse (ARFI) imaging technique. They found a significant difference in shear wave velocity between fetal growth restriction (FGR) placentas and normal placentas—higher in the FGR group—but no significant difference between the normal group and a pregnancy-induced hypertension group. Using strain elastography, Cimsit et al (71) found that the strain ratio was higher in patients with early-onset preeclampsia than in those with normal pregnancies.

ASL MR imaging monitors the delivery of labeled arterial blood water to tissues of interest. Gowland et al (72) used this technique in the study of human placentas and found values of normal placental perfusion of 176 mL/100 mg/min ± 96. Francis et al (73) found more areas of low perfusion related to a decrease in placental perfusion in IUGR pregnancies.

BOLD MR imaging provides information about tissue oxygenation and is based on the magnetic properties of hemoglobin. Sørensen et al (74) found that on BOLD images, the normoxic placenta appeared heterogeneous, with darker areas located to the fetal side and brighter areas to the maternal side. During hyperoxia, the placenta became brighter, the placental structure became more homogeneous,

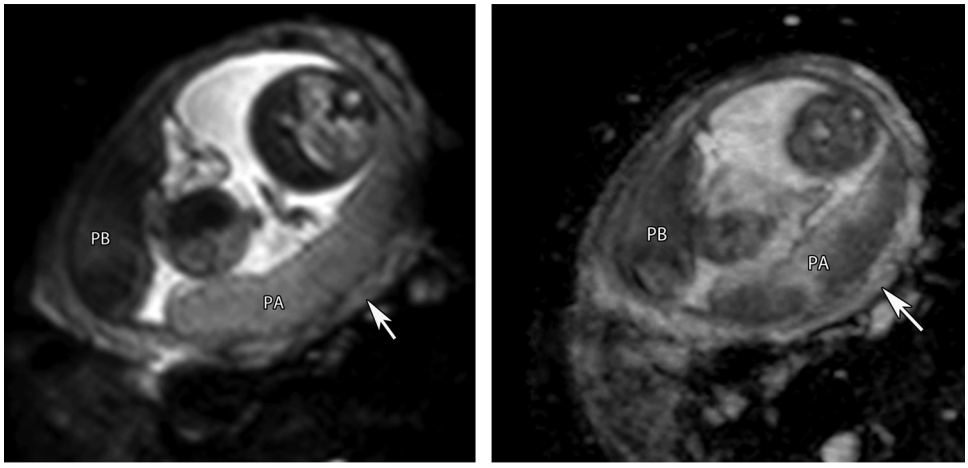

a. b.

Figure 26. Dichorionic diamniotic twin pregnancy with one fetus with IUGR at 18 weeks gestation. Axial diffusion-weighted image (b = 800 sec/mm^2) **(a)** and ADC map **(b)** show abnormal lower signal intensity in the placenta of twin B *(PB)* (smaller IUGR fetus) than in the placenta of twin A *(PA)* (normal fetus). The placenta of twin B also had a lower ADC value than the placenta of twin A (not shown). Note the difference in the signal intensity of the placenta compared with the myometrium (arrow), which allows delineation of the placental-myometrial interface.

Table 4: Features That Should Be Evaluated at US for Placental Evaluation

Criteria	Normal Placenta	Variations/Abnormalities
Morphology	Typically discoid with rounded margins	Succenturiate or bilobed Circumvallate placenta Placenta membranacea
Placental thickness	Typically 2–4 cm, correlating with gestational age	Thick or thin placenta
US echogenicity	Homogeneous	Venous lakes can be seen in normal placenta Calcifications Placental lacunae can be seen in MAP
Location	Variable	Low-lying placenta or placenta previa
Cord origin	Central	Marginal or velamentous cord insertion
Abnormal placental adherence	Retroplacental (subplacental) hypoechoic zone Smooth echogenic uterine serosa–bladder interface	Placenta accreta, increta, or percreta
Hematoma	Absent	Placental abruption and associated hematomas
Masses	Absent	Trophoblastic and nontrophoblastic tumors

and the BOLD signal of the total placenta increased ($\Delta BOLD_{tot}$, 15.2% ± 3.2 [mean ± standard deviation], $P < .0001$). They also found that during maternal hyperoxia, there was an increase in oxygenation in a number of human fetal organs, but the oxygenation of the fetal brain remained constant; thus, a "reversed" brain-sparing mechanism could be considered in healthy fetuses subjected to hyperoxia (75).

DWI has been implemented in human placentas, similar to its routine use in many other structures in the human body. Placental values of apparent diffusion coefficient (ADC) have been calculated for both normal pregnancies and pregnancies complicated by IUGR and preeclampsia, with an average ADC value of 1.77×10^{-3} mm^2 · sec^{-1} ± 0.19 (76); however, there is considerable variation in these values with gestational age. In IUGR placentas, ADC appears significantly decreased compared with normal pregnancies (77,78) (Fig 26).

Practical Evaluation of Placenta at Imaging

Placental evaluation is integrated as part of the routine prenatal US evaluation, in which systematic evaluation of the placenta is important (17). Table 4 is a list of the placental features that should be evaluated at US.

MR imaging is usually reserved as a complementary and problem-solving tool in placental evaluation. It demonstrates good delineation of the placental-myometrial interface at T2-weighted imaging and DWI, which is of value for diagnosis of MAP (12,13,53); however, MR imaging diagnosis of placental invasion remains challenging, and MR imaging should be reserved for the setting where there is high clinical suspicion with negative or equivocal US findings (12). Furthermore, MR imaging demonstrates well the zonal anatomy of the uterus, which is helpful in cases of PTN (14).

CT is reserved for selected circumstances, particularly trauma, where the clinical benefits of detecting maternal and fetal injuries outweigh the risk of fetal radiation exposure (16). CT is also used for evaluation of metastases in the setting of PTN (15).

Conclusion

The placenta has a crucial role throughout fetal development. The fetus completely depends on the placenta to survive; therefore, pathologic conditions associated with the placenta directly affect fetal morbidity and mortality. Systematic evaluation of the placenta during routine prenatal US should be performed to exclude pathologic conditions. MR imaging is reserved for equivocal cases, mainly for placental adherence abnormalities, while CT has a limited role in placental evaluation. Familiarity of radiologists with these various placental pathologic conditions is vital for alerting referring clinicians regarding the need for prompt and appropriate maternal and fetal management.

***Disclosures of Conflicts of Interest.*—M.D.** *Activities related to the present article:* disclosed no relevant relationships. *Activities not related to the present article:* grants from GE Healthcare and Philips Medical Imaging. *Other activities:* disclosed no relevant relationships.

References

1. Pinar H. The human placenta: normal developmental biology. Warwick, RI: Core Curriculum Publishers, 2009; 41–203.
2. Moore KL. The developing human: clinically oriented embryology. 8th ed. Philadelphia, Pa: Saunders/Elsevier, 2008; 55–135.
3. Jauniaux E, Ramsay B, Campbell S. Ultrasonographic investigation of placental morphologic characteristics and size during the second trimester of pregnancy. Am J Obstet Gynecol 1994;170(1 Pt 1):130–137.
4. Kanne JP, Lalani TA, Fligner CL. The placenta revisited: radiologic-pathologic correlation. Curr Probl Diagn Radiol 2005;34(6):238–255.
5. Elsayes KM, Trout AT, Friedkin AM, et al. Imaging of the placenta: a multimodality pictorial review. RadioGraphics 2009;29(5):1371–1391.
6. Kuo PL, Lin CC, Lin YH, Guo HR. Placental sonolucency and pregnancy outcome in women with elevated second trimester serum alpha-fetoprotein levels. J Formos Med Assoc 2003;102(5):319–325.
7. Kusanovic JP, Romero R, Gotsch F, et al. Discordant placental echogenicity: a novel sign of impaired placental perfusion in twin-twin transfusion syndrome? J Matern Fetal Neonatal Med 2010;23(1):103–106.
8. Raio L, Ghezzi F, Cromi A, Nelle M, Dürig P, Schneider H. The thick heterogeneous (jellylike) placenta: a strong predictor of adverse pregnancy outcome. Prenat Diagn 2004;24(3):182–188.
9. Grannum PA, Berkowitz RL, Hobbins JC. The ultrasonic changes in the maturing placenta and their relation to fetal pulmonic maturity. Am J Obstet Gynecol 1979;133(8):915–922.
10. Chen KH, Chen LR, Lee YH. Exploring the relationship between preterm placental calcification and adverse maternal and fetal outcome. Ultrasound Obstet Gynecol 2011;37(3):328–334.
11. Allen BC, Leyendecker JR. Placental evaluation with magnetic resonance. Radiol Clin North Am 2013;51(6):955–966.
12. Blaicher W, Brugger PC, Mittermayer C, et al. Magnetic resonance imaging of the normal placenta. Eur J Radiol 2006;57(2):256–260.
13. Rahaim NS, Whitby EH. The MRI features of placental adhesion disorder and their diagnostic significance: systematic review. Clin Radiol 2015;70(9):917–925.
14. Zaidi SF, Moshiri M, Osman S, et al. Comprehensive imaging review of abnormalities of the placenta. Ultrasound Q 2016;32(1):25–42.
15. Kani KK, Lee JH, Dighe M, Moshiri M, Kolokythas O, Dubinsky T. Gestational trophoblastic disease: multimodality imaging assessment with special emphasis on spectrum of abnormalities and value of imaging in staging and management of disease. Curr Probl Diagn Radiol 2012;41(1):1–10.
16. Wei SH, Helmy M, Cohen AJ. CT evaluation of placental abruption in pregnant trauma patients. Emerg Radiol 2009;16(5):365–373.
17. Abramowicz JS, Sheiner E. Ultrasound of the placenta: a systematic approach. I. Imaging. Placenta 2008;29(3):225–240.
18. Taniguchi H, Aoki S, Sakamaki K, et al. Circumvallate placenta: associated clinical manifestations and complications—a retrospective study. Obstet Gynecol Int 2014;2014:986230.
19. Arlicot C, Herve P, Simon E, Perrotin F. Three-dimensional surface rendering of the chorionic placental plate: the "tire" sign for the diagnosis of a circumvallate placenta. J Ultrasound Med 2012;31(2):340–341.
20. McCarthy J, Thurmond AS, Jones MK, et al. Circumvallate placenta: sonographic diagnosis. J Ultrasound Med 1995;14(1):21–26.
21. Shen O, Golomb E, Lavie O, Goldberg Y, Eitan R, Rabinowitz RR. Placental shelf: a common, typically transient and benign finding on early second-trimester sonography. Ultrasound Obstet Gynecol 2007;29(2):192–194.
22. Ekoukou D, Ng Wing Tin L, Nere MB, Bourdet O, Elalaoui Y, Bazin C. Placenta membranacea: review of the literature, a case report [in French]. J Gynecol Obstet Biol Reprod (Paris) 1995;24(2):189–193.
23. Lee AJ, Bethune M, Hiscock RJ. Placental thickness in the second trimester: a pilot study to determine the normal range. J Ultrasound Med 2012;31(2):213–218.
24. Elchalal U, Ezra Y, Levi Y, et al. Sonographically thick placenta: a marker for increased perinatal risk—a prospective cross-sectional study. Placenta 2000;21(2-3):268–272.
25. Reddy UM, Abuhamad AZ, Levine D, Saade GR; Fetal Imaging Workshop Invited Participants. Fetal imaging: executive summary of a joint Eunice Kennedy Shriver National Institute of Child Health and Human Development, Society for Maternal-Fetal Medicine, American Institute of Ultrasound in Medicine, American College of Obstetricians and Gynecologists, American College of Radiology, Society for Pediatric Radiology, and Society of Radiologists in Ultrasound fetal imaging workshop. J Ultrasound Med 2014;33(5):745–757.
26. Farine D, Peisner DB, Timor-Tritsch IE. Placenta previa: is the traditional diagnostic approach satisfactory? J Clin Ultrasound 1990;18(4):328–330.
27. Lauria MR, Smith RS, Treadwell MC, et al. The use of second-trimester transvaginal sonography to predict placenta previa. Ultrasound Obstet Gynecol 1996;8(5):337–340.
28. Mustafá SA, Brizot ML, Carvalho MH, Watanabe L, Kahhale S, Zugaib M. Transvaginal ultrasonography in predicting placenta previa at delivery: a longitudinal study. Ultrasound Obstet Gynecol 2002;20(4):356–359.
29. Dashe JS, McIntire DD, Ramus RM, Santos-Ramos R, Twickler DM. Persistence of placenta previa according to gestational age at ultrasound detection. Obstet Gynecol 2002;99(5 Pt 1):692–697.

30. Di Salvo DN, Benson CB, Laing FC, Brown DL, Frates MC, Doubilet PM. Sonographic evaluation of the placental cord insertion site. AJR Am J Roentgenol 1998;170(5):1295–1298.
31. Liu CC, Pretorius DH, Scioscia AL, Hull AD. Sonographic prenatal diagnosis of marginal placental cord insertion: clinical importance. J Ultrasound Med 2002;21(6):627–632.
32. Kellow ZS, Feldstein VA. Ultrasound of the placenta and umbilical cord: a review. Ultrasound Q 2011;27(3):187–197.
33. Society of Maternal-Fetal (SMFM) Publications Committee, Sinkey RG, Odibo AO, Dashe JS. #37: diagnosis and management of vasa previa. Am J Obstet Gynecol 2015;213(5):615–619.
34. Catanzarite V, Oyelese Y. Diagnosis and management of vasa previa. Am J Obstet Gynecol 2016;214(6):764.
35. Moshiri M, Zaidi SF, Robinson TJ, et al. Comprehensive imaging review of abnormalities of the umbilical cord. RadioGraphics 2014;34(1):179–196.
36. Thompson MO, Vines SK, Aquilina J, Wathen NC, Harrington K. Are placental lakes of any clinical significance? Placenta 2002;23(8-9):685–690.
37. Oyelese Y, Ananth CV. Placental abruption. Obstet Gynecol 2006;108(4):1005–1016.
38. Glantz C, Purnell L. Clinical utility of sonography in the diagnosis and treatment of placental abruption. J Ultrasound Med 2002;21(8):837–840.
39. Masselli G, Brunelli R, Di Tola M, Anceschi M, Gualdi G. MR imaging in the evaluation of placental abruption: correlation with sonographic findings. Radiology 2011;259(1):222–230.
40. Sadro C, Bernstein MP, Kanal KM. Imaging of trauma. II. Abdominal trauma and pregnancy: a radiologist's guide to doing what is best for the mother and baby. AJR Am J Roentgenol 2012;199(6):1207–1219.
41. Lowdermilk C, Gavant ML, Qaisi W, West OC, Goldman SM. Screening helical CT for evaluation of blunt traumatic injury in the pregnant patient. RadioGraphics 1999;19(Spec No):S243–S255; discussion S256–S258.
42. Saphier NB, Kopelman TR. Traumatic Abruptio Placenta Scale (TAPS): a proposed grading system of computed tomography evaluation of placental abruption in the trauma patient. Emerg Radiol 2014;21(1):17–22.
43. Manriquez M, Srinivas G, Bollepalli S, Britt L, Drachman D. Is computed tomography a reliable diagnostic modality in detecting placental injuries in the setting of acute trauma? Am J Obstet Gynecol 2010;202(6):611.e1–611.e5.
44. Jain V, Chari R, Maslovitz S, et al. Guidelines for the management of a pregnant trauma patient. J Obstet Gynaecol Can 2015;37(6):553–574.
45. Tantbirojn P, Crum CP, Parast MM. Pathophysiology of placenta creta: the role of decidua and extravillous trophoblast. Placenta 2008;29(7):639–645.
46. Strickland S, Richards WG. Invasion of the trophoblasts. Cell 1992;71(3):355–357.
47. Collins SL, Ashcroft A, Braun T, et al. Proposal for standardized ultrasound descriptors of abnormally invasive placenta (AIP). Ultrasound Obstet Gynecol 2016;47(3):271–275.
48. Hull AD, Moore TR. Multiple repeat cesareans and the threat of placenta accreta: incidence, diagnosis, management. Clin Perinatol 2011;38(2):285–296.
49. Comstock CH, Bronsteen RA. The antenatal diagnosis of placenta accreta. BJOG 2014;121(2):171–181; discussion 181–182.
50. Comstock CH, Love JJ Jr, Bronsteen RA, et al. Sonographic detection of placenta accreta in the second and third trimesters of pregnancy. Am J Obstet Gynecol 2004;190(4):1135–1140.
51. Cali G, Giambanco L, Puccio G, Forlani F. Morbidly adherent placenta: evaluation of ultrasound diagnostic criteria and differentiation of placenta accreta from percreta. Ultrasound Obstet Gynecol 2013;41(4):406–412.
52. Wong HS, Cheung YK, Zuccollo J, Tait J, Pringle KC. Evaluation of sonographic diagnostic criteria for placenta accreta. J Clin Ultrasound 2008;36(9):551–559.
53. Morita S, Ueno E, Fujimura M, Muraoka M, Takagi K, Fujibayashi M. Feasibility of diffusion-weighted MRI for defining placental invasion. J Magn Reson Imaging 2009;30(3):666–671.
54. Duan XH, Wang YL, Han XW, et al. Caesarean section combined with temporary aortic balloon occlusion followed by uterine artery embolisation for the management of placenta accreta. Clin Radiol 2015;70(9):932–937.
55. Cali G, Forlani F, Giambanco L, et al. Prophylactic use of intravascular balloon catheters in women with placenta accreta, increta and percreta. Eur J Obstet Gynecol Reprod Biol 2014;179:36–41.
56. Allen SD, Lim AK, Seckl MJ, Blunt DM, Mitchell AW. Radiology of gestational trophoblastic neoplasia. Clin Radiol 2006;61(4):301–313.
57. Berkowitz RS, Goldstein DP. Clinical practice: molar pregnancy. N Engl J Med 2009;360(16):1639–1645.
58. Jain KA. Gestational trophoblastic disease: pictorial review. Ultrasound Q 2005;21(4):245–253.
59. Ngan HY, Bender H, Benedet JL, et al. Gestational trophoblastic neoplasia: FIGO 2000 staging and classification. Int J Gynaecol Obstet 2003;83(suppl 1):175–177.
60. Himoto Y, Kido A, Minamiguchi S, et al. Prenatal differential diagnosis of complete hydatidiform mole with a twin live fetus and placental mesenchymal dysplasia by magnetic resonance imaging. J Obstet Gynaecol Res 2014;40(7):1894–1900.
61. Wentworth P. The incidence and significance of haemangioma of the placenta. J Obstet Gynaecol Br Commonw 1965;72:81–88.
62. Wallenburg HC. Chorioangioma of the placenta: thirteen new cases and a review of the literature from 1939 to 1970 with special reference to the clinical complications. Obstet Gynecol Surv 1971;26(6):411–425.
63. Zalel Y, Weisz B, Gamzu R, Schiff E, Shalmon B, Achiron R. Chorioangiomas of the placenta: sonographic and Doppler flow characteristics. J Ultrasound Med 2002;21(8):909–913.
64. Zalel Y, Gamzu R, Weiss Y, et al. Role of color Doppler imaging in diagnosing and managing pregnancies complicated by placental chorioangioma. J Clin Ultrasound 2002;30(5):264–269.
65. Zanardini C, Papageorghiou A, Bhide A, Thilaganathan B. Giant placental chorioangioma: natural history and pregnancy outcome. Ultrasound Obstet Gynecol 2010;35(3):332–336.
66. Taori K, Patil P, Attarde V, Singh A, Rangankar V. Chorioangioma of placenta: sonographic features. J Clin Ultrasound 2008;36(2):113–115.
67. Ahmed N, Kale V, Thakkar H, Hanchate V, Dhargalkar P. Sonographic diagnosis of placental teratoma. J Clin Ultrasound 2004;32(2):98–101.
68. Altman JF, Lowe L, Redman B, et al. Placental metastasis of maternal melanoma. J Am Acad Dermatol 2003;49(6):1150–1154.
69. Wu S, Nan R, Li Y, Cui X, Liang X, Zhao Y. Measurement of elasticity of normal placenta using the Virtual Touch quantification technique. Ultrasonography 2016;35(3):253–257.
70. Sugitani M, Fujita Y, Yumoto Y, et al. A new method for measurement of placental elasticity: acoustic radiation force impulse imaging. Placenta 2013;34(11):1009–1013.
71. Cimsit C, Yoldemir T, Akpinar IN. Strain elastography in placental dysfunction: placental elasticity differences in normal and preeclamptic pregnancies in the second trimester. Arch Gynecol Obstet 2015;291(4):811–817.
72. Gowland PA, Francis ST, Duncan KR, et al. In vivo perfusion measurements in the human placenta using echo planar imaging at 0.5 T. Magn Reson Med 1998;40(3):467–473.
73. Francis ST, Duncan KR, Moore RJ, Baker PN, Johnson IR, Gowland PA. Non-invasive mapping of placental perfusion. Lancet 1998;351(9113):1397–1399.
74. Sørensen A, Peters D, Fründ E, Lingman G, Christiansen O, Uldbjerg N. Changes in human placental oxygenation during maternal hyperoxia estimated by blood oxygen level-dependent magnetic resonance imaging (BOLD MRI). Ultrasound Obstet Gynecol 2013;42(3):310–314.
75. Sørensen A, Peters D, Simonsen C, et al. Changes in human fetal oxygenation during maternal hyperoxia as estimated by BOLD MRI. Prenat Diagn 2013;33(2):141–145.
76. Bonel HM, Stolz B, Diedrichsen L, et al. Diffusion-weighted MR imaging of the placenta in fetuses with placental insufficiency. Radiology 2010;257(3):810–819.
77. Gowland P. Placental MRI. Semin Fetal Neonatal Med 2005;10(5):485–490.
78. Derwig I, Lythgoe DJ, Barker GJ, et al. Association of placental perfusion, as assessed by magnetic resonance imaging and uterine artery Doppler ultrasound, and its relationship to pregnancy outcome. Placenta 2013;34(10):885–891.